Cell

Segregation of Protein Aggregates Involves Actin and the Polarity Machinery

Cells of yeast to mammals have evolved the means of spatial quality control (SQC), which includes the transport of protein aggregates on microtubules into a structure called the aggresome (Kopito, 2000; Wang et al., 2009) and a factor-dependent compartmentalization of aggregates into juxtanuclear sites (JUNQ) and perivacuolar inclusions (IPOD) (Kaganovich et al., 2008). SQC also encompasses an actin cytoskeleton-, polarisome-, and Hsp104-dependent segregation of damaged proteins during yeast cytokinesis (Aguilaniu et al., 2003; Erjavec et al., 2007; Tessarz et al., 2009). In addition, some aggregates in yeast daughter cells were observed to move (retrograde) into the mother cell after a transient heat stress (Liu et al., 2010). In this issue of *Cell*, Zhou et al. (2011) now extend this analysis and, with the aid of theoretical simulations, suggest that motility of protein aggregates is characterized by random and slow diffusion, completely devoid of directional bias. Further, it is argued that aggregate asymmetry is established in a purely passive and random manner and that no active, factor-dependent (e.g., polarisome) mechanism is involved in conferring SQC. This model contrasts that of Tessarz et al., (2009) and Liu et al., (2010), which both interpret the failure of mutants with defects in polarisome and Hsp104 functions to establish damage asymmetry indicative of damage retention being a factor-dependent process.

When considering the different views on the establishment of damage asymmetry, it should be pointed out that measurements aimed at determining the frequency of aggregate movement between mother and daughter should only include budding events in which such transfer is physically possible. This is the case during the S to early G2 phase, when the polarisome is localized at the bud tip and actin cables extend from the bud into the mother compartment. When these phases are considered, our data show that there is a bias toward retrograde movement of aggregates from daughter to mother. In 393 budding events analyzed (between 56 and 84 such events were analyzed in the Zhou et al. study), we found that 15.5% showed cross-compartment movements (Figure 1A), and among these, retrograde movement from bud to mother (66.5%) is significantly more frequent than anterograde movement (25.4%; $p = 0.03$) and movement in both directions (8.1%; $p = 0.007$) (Figure 1B). Figure S1 in the Supplemental Information available online shows two budding events with simultaneously retrograde movement of aggregates (Movie S1 is an uncropped full-field movie showing several retrograde movements).

Analyzing cells harboring the ATPase-negative Hsp104^{Y662A}-GFP variant, in which aggregates are stable, demonstrated that some aggregates form elongated, fibrillar structures (Figure 1C, red arrows). The end (yellow arrow, top) of this structure moved toward the end of the mother cell in a manner that is not compatible with stochastic diffusion (Movies S2 and S3). Moreover, we used the Abp140-3GFP fusion (Buttery et al., 2007) in the Hsp104^{Y662A}-mCherry strain to test whether the aggregates colocalize with the actin cytoskeleton. Abp140 binds to actin cables and forms focal nodes that have been used previously to visualize retrograde movement of actin cables (Yang and Pon, 2002). Using three-dimensional (3D) imaging, we found that the Hsp104^{Y662A}-mCherry fibrillar aggregates colocalize with Abp140-3GFP (Figure 1D). As the actin cytoskeleton does not diffuse randomly, it is implausible that the aggregates associated with these structures diffuse in a factor-independent and random walk-type manner within the cells.

To test further the involvement of the polarisome formin Bni1 in aggregate segregation, we used the aggregation-prone Huntington's disease protein Htt103Q-GFP and an experimental setup that removes the drawback of a heat shock, which causes a complete, transient breakdown of actin cables (see Figure 1E). Analyzing the inheritance of all visible Htt103Q foci, small and large, demonstrated that yeast mother cells effectively retained Htt103Q aggregates during cytokinesis (Figures 1F and 1G) and that the absence of Bni1 significantly reduced this retention capacity (Figure 1G; $p = 3.42 \times 10^{-5}$). Thus, we find that the segregation of both aggregation-prone disease proteins and indigenous heat-induced Hsp104-containing aggregates (Liu et al., 2010) are dependent on the polarisome. Zhou et al. report that cells lacking the formin Bnr1 display an increased aggregate diffusion after a transient heat shock that, in fact, would be predicted to cause a reduced retention of aggregates by their simulation model (a similar prediction could be made for Bni1-deficient cells, as the bud neck of such cells is much wider than the wild-type). Yet, no alteration in aggregate retention could be detected by their experimental approach. In addition, the experimental analysis of aggregate diffusion in cells treated with latranculin A and cells deleted for *BNR1* unexpectedly indicated that these well-known means of reducing actin cable formation have the exact opposite effect on aggregate movement, decreasing and increasing diffusion, respectively (Zhou et al., 2011). Such confounding results make it difficult to evaluate the usefulness of the model and simulations provided.

In relation to the data presented here and in Zhou et al., it should be emphasized that the most likely mechanism underlying aggregate asymmetry during aging of yeast cells is the result of aggregates not entering the daughter cell in the first place. We have previously suggested "that actin cables may provide a scaffold for large Hsp104 containing aggregates" and "that aggregates tethered on cables will not enter the buds" (Liu et al., 2010). That aggregate asymmetry during cytokinesis of unstressed cells is predominantly due to daughters clearing themselves of aggregates by retrograde movement would mean that most daughters first inherit aggregates from the mother by forward movement

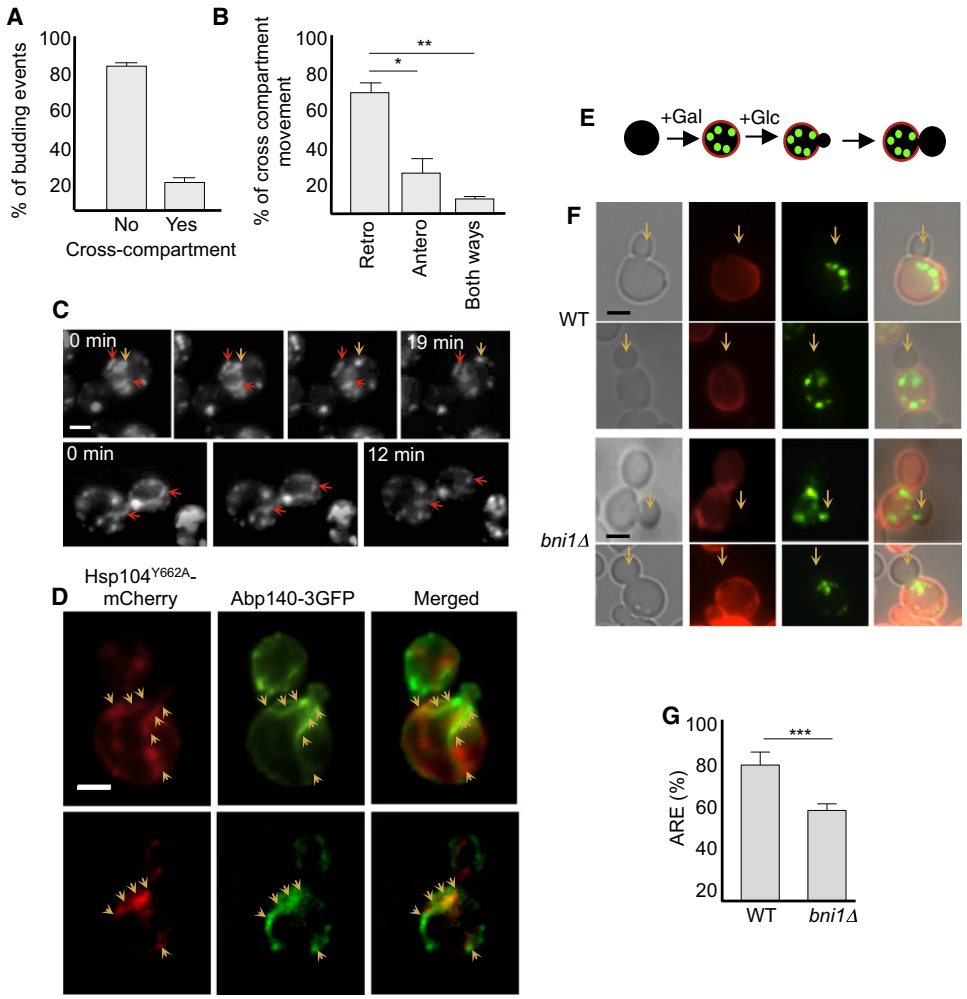

Figure 1. Transport of Protein Aggregates between Mother and Daughter Cells and Requirement for Bni1 in the Segregation of Huntingtin Htt103Q Aggregates

(A and B) Quantification of aggregate movement between mother and daughter cells. Data are represented as mean ± standard deviation (SD). *p = 0.03; **p = 0.007.

(C) Stable fibrillar Hsp104^{Y662A}-GFP structures (red arrows) observed within cells in later cell-cycle stages. Top panel shows a cell with middle-sized buds (G2-M phase). Yellow arrow indicates the end of the fibrillar structure extending to the end of the mother cell. Bottom panel shows an M-G1 phase cell, which forms fibrillar aggregate structures along the bud-mother axis in both mother and daughter compartments. Scale bars, 2 μm.

(D) Colocalization of Hsp104^{Y662A}-GFP fibrillar aggregates and Abp140-3GFP (yellow arrows). Scale bars, 2 μm.

(E) Schematic representation of the experimental design for segregation of HttQ103-GFP. HttQ103-GFP aggregation was triggered by inducing the corresponding gene by galactose. Expression was subsequently turned off by adding glucose and segregation scored during the next budding event. Mother cells were stained briefly with concanavalin A (red circle in the picture), allowing easy identification of new buds (not stained).

(F) Pictures of wild-type and *bni1Δ* cells displaying new budding events (yellow arrows) after the turn-off of HttQ103-GFP aggregate production. Pictures from left to right are bright field, Concanavalin A-Alexa Fluor 647, HttQ103-GFP, and merged images. Scale bars, 2 μm.

(G) Quantification of aggregate retention efficiency (ARE) in wild-type and *bni1Δ* cells. 551 and 650 budding events were counted for wild-type and *bni1Δ*, respectively, and two individual clones were tested for each strain. Data are represented as mean ± SD. ***p = 3.42 × 10^{-5}.

followed by retrograde transport back to the mother. We do not believe nor suggest (Liu et al., 2010) that this is a likely explanation for generating damage-free daughter cells, and stating that our model is suggesting that retrograde transport is the major reason for creating damage asymmetry is inaccurate and misleading. That aggregate resolution can take place in daughter cells is obvious and has been shown previously, but this process alone cannot explain the unequal inheritance of damage and was not approached in the Liu et al. (2010) study.

Finally, the notion of Zhou et al. of aggregates moving and being partitioned within the cells by only random, factor-independent diffusion is in conflict with a number of reports relating to aggregate partitioning between different compartments, e.g., JUNQ and IPOD, and the formation of aggresomes (e.g., Kaganovich et al., 2008; Wang et al., 2009; Kopito 2000). These contributions demonstrate that protein aggregates associate, in a factor-dependent manner (e.g., ubiquitin), with different cellular constituents,

including juxtanuclear proteasome-enriched sites, vacuoles in the mother cell periphery, endosomal machineries, microtubules, and spindle pole bodies. The data presented herein show that Hsp104-containing aggregates, like prion aggregates (Chernova et al., 2011), also associate with the actin cytoskeleton. It is difficult to understand how all such aggregates disperse within the cell by random diffusion, as suggested by Zhou et al., considering their association with different cellular structures that themselves do not diffuse in such a manner. Therefore, we consider it necessary to perform aggregate diffusion analysis also under conditions that do not include a heat shock and transient breakdown of the cytoskeleton. As reported herein, such an approach confirms the involvement of Bni1 in establishing aggregate asymmetry. We maintain the view that the experimental data available are consistent with aggregate compartmentalization and segregation relying on factor-dependent mechanisms and envision that the genome-wide screens initiated to identify such factors will shed further light on the processes involved.

SUPPLEMENTAL INFORMATION

Supplemental Information includes Extended Experimental Procedures, one figure, one table, and three movies and can be found with this article online at doi:10.1016/j.cell.2011.11.018.

ACKNOWLEDGMENTS

This work was supported by grants from the Swedish Natural Research Council (VR) and the Knut and Alice Wallenberg Foundation (Wallenberg Scholar) to T.N., the Science Faculty of the University of Gothenburg and Signhild Engkvists (SE) Foundation to B.L., the Flemish Society of Alzheimer Research (SAO) to V.F., as well as IWT-Vlaanderen (SBO Neuro-Target and Baekeland), the KULeuven Research Fund, and the Fund of Scientific Research of Flanders (FWO), Belgium, to J.W. We thank Rong Li for providing Hsp104^{Y662A}-GFP and David Pellman for providing Abp140-3GFP and valuable suggestions.

Beidong Liu,[1,3,*] Lisa Larsson,[1] Vanessa Franssens,[2] Xinxin Hao,[1] Sandra Malmgren Hill,[1] Veronica Andersson,[1] Daniel Höglund,[1] Jia Song,[3] Xiaoxue Yang,[3] David Öling,[1] Julie Grantham,[1] Joris Winderickx,[2] and Thomas Nyström[1,*]

[1]Department of Cell and Molecular Biology, University of Gothenburg, Medicinaregatan 9C, 413 90 Göteborg, Sweden

[2]Functional Biology, Katholieke Universiteit Leuven, Kasteelpark Arenberg 31, 3001 Heverlee, Belgium

[3]Department of Life Science and Engineering, Harbin Institute of Technology, Harbin 150001, China

*Correspondence: beidong.liu@cmb.gu.se (B.L.), thomas.nystrom@cmb.gu.se (T.N.)

DOI 10.1016/j.cell.2011.11.018

REFERENCES

Aguilaniu, H., Gustafsson, L., Rigoulet, M., and Nyström, T. (2003). Science *299*, 1751–1753.

Buttery, S.M., Yoshida, S., and Pellman, D. (2007). Mol. Biol. Cell *18*, 1826–1838.

Chernova, T.A., Romanyuk, A.V., Karpova, T.S., Shanks, J.R., Ali, M., Moffatt, N., Howie, R.L., O'Dell, A., McNally, J.G., Liebman, S.W., et al. (2011). Mol. Cell *43*, 242–252.

Erjavec, N., Larsson, L., Grantham, J., and Nyström, T. (2007). Genes Dev. *21*, 2410–2421.

Kaganovich, D., Kopito, R., and Frydman, J. (2008). Nature *454*, 1088–1095.

Kopito, R.R. (2000). Trends Cell Biol. *10*, 524–530.

Liu, B., Larsson, L., Caballero, A., Hao, X., Oling, D., Grantham, J., and Nyström, T. (2010). Cell *140*, 257–267.

Tessarz, P., Schwarz, M., Mogk, A., and Bukau, B. (2009). Mol. Cell. Biol. *29*, 3738–3745.

Wang, Y., Meriin, A.B., Zaarur, N., Romanova, N.V., Chernoff, Y.O., Costello, C.E., and Sherman, M.Y. (2009). FASEB J. *23*, 451–463.

Yang, H.C., and Pon, L.A. (2002). Proc. Natl. Acad. Sci. USA *99*, 751–756.

Zhou, C., Slaughter, B.D., Unruh, J.R., Eldakak, A., Rubinstein, B., and Li, R. (2011). Cell *147*, this issue, 1186–1196.